JOURNAL OF MATERIALS SCIENCE 36 (2001) 757–766

Microstructural study of co-electroplated Au/Sn alloys

W. SUN, D. G. IVEY
Department of Chemical and Materials Engineering, University of Alberta, Edmonton, Alberta, T6G 2G6 Canada
E-mail: divey@accessweb.com

Gold-tin eutectic solder (20 wt% Sn), because of its excellent mechanical and thermal properties, is utilized for flip chip and laser bonding in optoelectronic applications. Coelectroplating of Au and Sn has been investigated as an alternative to conventional methods for depositing Au/Sn alloys. Pulse current (PC) and direct current (DC) plating tests have been performed and compared using a suitably stable plating solution. Plating conditions, including current density and ON and OFF times (for PC plating), have been varied to optimize the process. Reproducibility tests have also been performed. It is shown that a range of alloy compositions can be deposited, including eutectic and near-eutectic compositions, with compositional and microstructural uniformity potentially suitable for microelectronic and optoelectronic solder applications.
© 2001 Kluwer Academic Publishers

1. Introduction

In electronic/optoelectronic packaging, chip bonding serves three major functions, i.e., mechanical support, heat dissipation and electrical connection. The choice of solder material for bonding is based on optimization of a number of properties, including solderability, melting temperature, Young's modulus (or stiffness), coefficient of thermal expansion, Poisson's ratio, fatigue life, creep rate and corrosion resistance. In terms of melting temperature, solders are typically classified as either hard (high melting temperature) or soft (low melting temperature). The Pb/Sn system is an example of a soft solder, which is commonly used for electronic packaging. Hard solders, e.g., Au/Sn, are used for optoelectronic packaging. Au-20 wt% Sn, which corresponds to the Au-rich eutectic composition, is the most common composition utilized; it has a relatively high melting temperature (280°C), good creep behaviour and good corrosion resistance.

Traditionally, solder preforms, paste or deposited solder have been used to bond microelectronic and photonic devices onto submounts. Solder preforms of eutectic Au-Sn are produced via a chill-block melt-spinning technique [1]. The high rate of heat extraction associated with this process causes the metal to solidify almost instantaneously, resulting in the formation of a thin strip of the alloy (20–50 μm thick) with an amorphous or microcrystalline structure. Preforms are problematic, however, in terms of handling and alignment and become impractical for fine-pitch and flip chip applications because of poor thickness and bonding area control. Preforms are also susceptible to oxidation prior to initiation of the bonding cycle.

Solder paste screen printing is a simple process with a low operating cost. The paste consists of Au-Sn powder and an organic binder. However, the solder particles are extremely susceptible to oxidation and solder contamination can result from organic decomposition during bonding.

Deposited solder offers advantages over the other two processes, such as decreased oxide formation prior to bonding and more accurate control of the solder thickness and volume [2]. The solder can be deposited using thin film technology, either vapour deposition or electron-beam deposition, using patterned photoresist or a shadow mask, or by electroplating. Electron beam evaporation is the most common method to sequentially deposit Au/Sn alternating layers, producing a multilayer stack with the desired composition [2–4]. Thermal evaporation has also been employed to deposit Au and Sn sequentially to a total thickness of about 2.5 μm [5, 6].

Co-evaporation of Au-Sn solder, using electron beam evaporation for the Au and resistive heating for the Sn, has also been reported [7]. Layers up to $\approx$3 μm in thickness at the eutectic composition have been deposited. Considerable heating of the substrate occurs during deposition, which requires that the process be interrupted to allow for cooling. This results in a very lengthy deposition process (more than several hours).

Electroplating of Au/Sn is attractive primarily because of its low cost and simplicity of operation. The technology for electroplating Au or Sn is quite well developed. Gold electroplating has a history dating back 150 years. Gold can be deposited from alkaline or acidic baths - the source of Au being primarily cyanides (e.g., $KAu(CN)_2$)) [8]. Non-cyanide electrolytes, such

as $KAuCl_4$ or gold sulphite, are other possible sources of Au. Studies on non-cyanide electrolytes have shown that these systems offer higher purity and freedom from breakdown, but are more sensitive to operating conditions and composition control. Electroplated Sn and Sn alloys are widely used in industrial applications. Examples of typical solutions include alkaline stannate solutions based on sodium or potassium stannate, acid Sn solutions based on stannous sulphate and acid fluorate solutions based on stannous fluoroborate.

Sequential electrodeposition of Au/Sn solder, using commercial Au and Sn plating baths, has been employed to fabricate Au/Sn bumps on patterned Si wafers with Au seed layers [9–11]. Gold is deposited first followed by Sn to a total thickness of up to $\approx$10 μm.

Interest in co-electroplating of Au-Sn alloys dates back several decades. However, only a few papers have been published. Available information concerning the coelectroplating of Au-Sn alloys is mainly confined to the patent literature [e.g., 12, 13]. A recent patent [12], employing a cyanide-based electrolyte, reported the deposition of bright Au-Sn deposits (at more than 0.1 μm thick) containing 75–95wt.% Au. A non-cyanide based electrolyte - Au and Sn were dissolved from chlorides - was reported in another patent [13]. A 7 μm thick Au-Sn alloy layer (20 ± 2 wt% Sn) was plated on a 50 mm Si wafer.

Other co-electroplating systems have been reported in the literature [14–17]. The main difficulties in coplating of Au-Sn alloys are two fold. First of all, it is difficult to control the deposition process. Not only must 2 metals be codeposited, but their compositions must be controlled. The other problem is continual oxidation of the stannous tin to stannic tin at anodes when insoluble anodes are used.

A suitable non-cyanide solution for co-depositing Au-Sn alloys over a range of compositions (including the eutectic) has been developed. The details of solution development will not be presented here, as the paper will focus on deposit structure, composition, uniformity and reproducibility. The primary aim of this paper is to demonstrate that Au-Sn alloys can be coelectroplated at compositions near the eutectic value and with suitable uniformity for subsequent bonding purposes. Deposition conditions are varied in an attempt to study their effect on deposit morphology. No bonding experiments are reported here.

2. Experimental methods

The electroplating setup consisted of a pulsed current supply, with ON and OFF time settings in the 0–9.9 ms range. A 50 Ω standard resistance R_O was connected in series with the plating bath to monitor the peak current density in the circuit through an oscilloscope. A non-cyanide (weakly acidic) plating solution of fixed composition was prepared from Au and Sn chloride salts, with appropriate stabilizers, buffering agents and levelers. An acidic plating solution is more compatible with photoresist developers, although if the acidity is too high hydrogen evolution becomes a problem. The cathodes were either InP or Si wafers, coated with Ti (25 nm)/Au (250 nm) blanket metallizations. Wafers were sectioned into smaller pieces, each having an exposed area $\approx$1 cm $\times$ 1 cm defined by stop-off lacquer. Platinum foil was used as the anode. The cathode-anode spacing was maintained at a fixed value throughout the plating process.

Plating experiments were carried out at a fixed temperature (20°C) under both direct current (DC) and pulsed current (PC) conditions. For PC plating, ON and OFF times were varied and their effects correlated with deposit composition and microstructure. One set of experiments was done at constant average current density (2.4 mA/cm^2), cycle period (10 ms) and plating time (1 hr), while varying the ON time from 0.2–5 ms. A second set of experiments was done while maintaining a constant peak curent density (10 mA/cm^2), OFF time (8 ms) and plating time (80 min), and varying the ON time from 0.5–4 ms. Finally, plating experiments were done at OFF times ranging from 3–9.9 ms. The peak current density was maintained at 10 mA/cm^2, with an ON time and plating time of 2 ms and 80 min respectively.

All electroplated samples were examined in a Hitachi S-2700 scanning electron microscope (SEM), equipped with a Link eXL energy dispersive x-ray (EDX) spectroscopy system. An accelerating voltage of 20 kV was used for both imaging and composition analysis; pure Au and pure Sn standards were used for quantitative analysis. Both plan view and cross section samples were examined. Cross sections were either prepared by cleaving, for imaging and thickness measurements, or by polishing, for quantitative composition analysis. Deposit surface roughness was measured by atomic force microscopy (Digital Instruments Nanoscope *E*).

Reproducibility tests were carried out to assess the repeatability of the plating bath. A single metallized InP wafer piece ($\approx$1.5 cm^2 exposed area) was plated continuously from a 50 ml plating solution. An average current density of 1.6 mA/cm^2 was used, with an ON time of 2 ms and an OFF time of 8 ms, for a total of 40 hrs. Deposit composition was determined from polished cross sections at 2.25 μm intervals from the deposit-wafer interface.

3. Results and discussion

3.1. DC vs PC plating

Deposit composition results for DC and PC (ON time of 2 ms and OFF time of 8 ms) plated samples are shown in Fig. 1. The composition vs current tendencies are similar for DC and PC plating. The Sn content initially increases with increasing average current density, reaches a plateau and then decreases with increasing current density. Increasing the current density tends to favour plating of the less noble metal (Sn in this case). If the current density is too high, however, hydrogen evolution becomes significant, decreasing the efficiency of alloy plating. Hydrogen evolution may also cause a local increase in pH, increasing the susceptibility of Sn ion complexing. Tin ions will be further stabilized as a result of complex formation, suppressing Sn plating and reducing tin concentration in the deposit.

From Fig. 1, it is clear that DC deposits obtained at the same current densities are consistently lower in

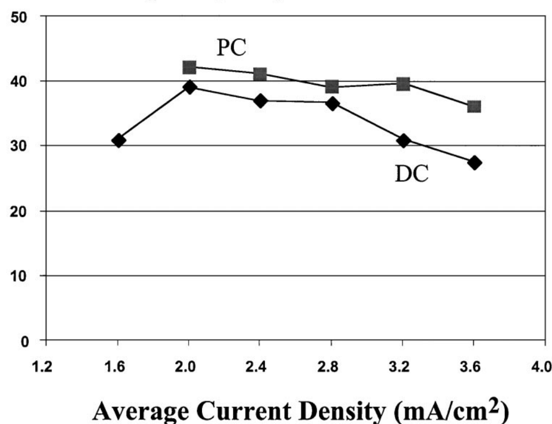

Figure 1 Deposit composition vs average current density for DC plating and PC plating. The ON and OFF times for PC plating are 2 ms and 8 ms respectively. Error bars are contained within the data points.

Sn content than PC deposits. This result is similar to that found in other Au alloy pulse plating systems, e.g., Au-Co and Au-Ni systems [18], and may be due to a difference in polarization behaviour for PC and DC modes. The cathodic potential in PC mode may be more negative relative to DC mode, which would favour Sn plating.

Representative microstructures for the deposition conditions presented in Fig. 1 are shown in Fig. 2. DC and PC deposits are similar for current densities in the 1.6–2.0 mA/cm^2 range, i.e., at low average current densities PC plating has no obvious influence on deposit microstructure. Both DC and PC deposits show a tendency towards coarser microstructures at higher current densities, with the effect more pronounced for DC deposits. At a given average current density, the peak current density is considerably higher for PC plating, i.e., about 5 times that for DC plating (based on a duty cycle of 20%). The higher peak current density results in higher overpotentials and a finer deposit structure, because the rate of electron transfer in PC deposits to form adatoms is much faster than the diffusion rate of the adatoms across the surface to positions in the lattice, which favours nucleation. Grain refinement has been observed in other PC systems, e.g., a phosphate gold plating bath [19]. If the current density is too high, the limiting value is exceeded, i.e., metal ions are consumed faster than they can arrive at the cathode and the plating is under diffusion control, resulting in dendritic growth and a rough deposit surface.

The diffusion layer in PC plating is considered to consist of a pulsating part and a stationary part [20]. After only a few current pulses the concentration fluctuations at the cathode become independent of the number of pulses applied. Depletion of the cation concentration in the pulsating diffusion layer limits the pulse current density, and depletion of the cation concentration in the outer diffusion layer limits the average current density. The thickness of the pulsating diffusion layer (δ_P) and

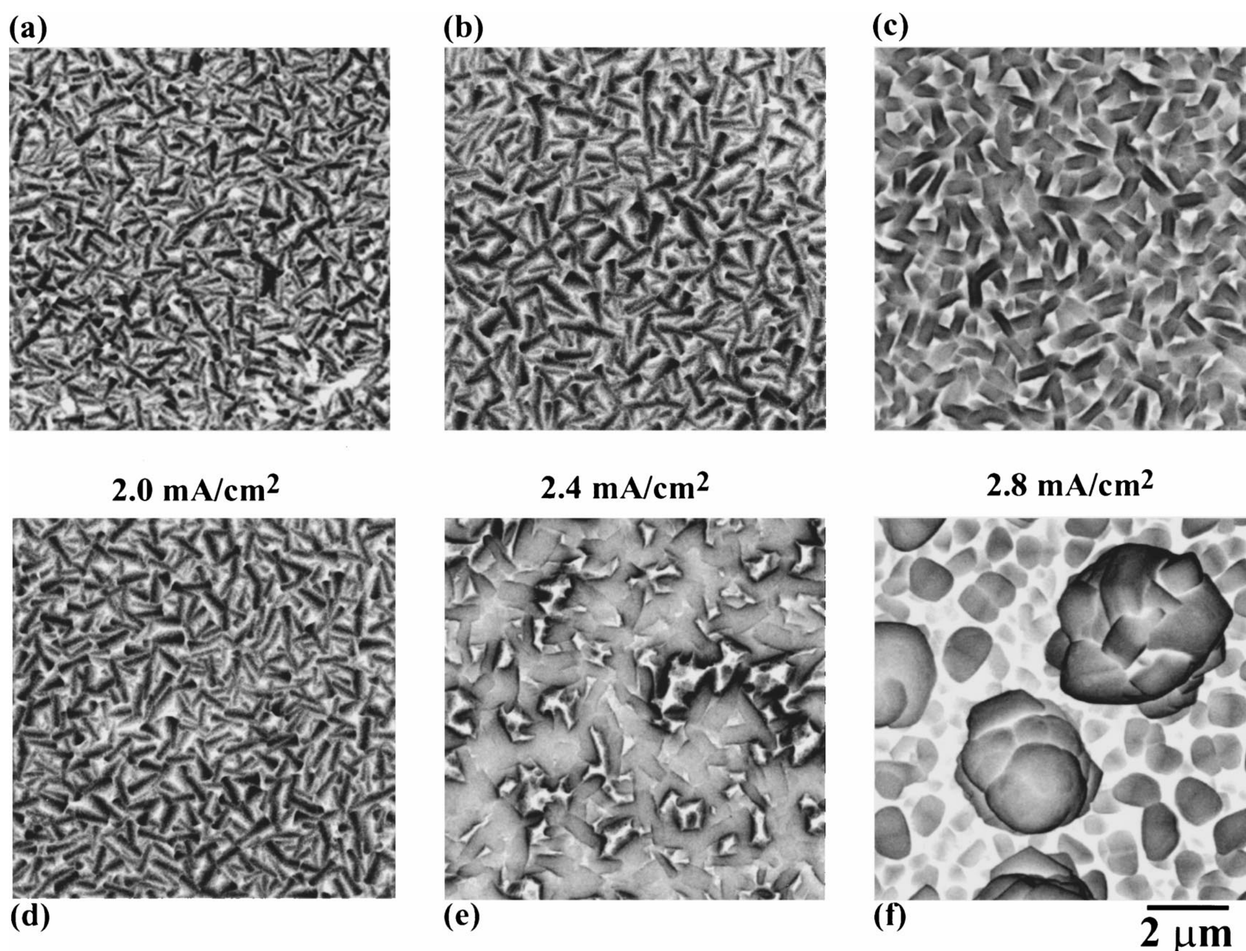

Figure 2 SEM secondary electron (SE), plan view images for PC plated deposits (a–c) and DC plated deposits (d–f). The ON and OFF times for PC plating are 2 ms and 8 ms respectively.

the pulse limiting current density (i_{LP}) depend on the ON time (t_{ON}), the duty cycle ($\gamma = t_{ON}/(t_{ON} + t_{OFF})$) and the diffusion coefficient (D). Both δ_P and i_{LP} increase with increasing ON time and D. Assuming a linear concentration profile through the pulsating diffusion layer:

$$\delta_P = [4/\pi D t_{ON}(1-\gamma)]^{0.5}$$
$$i_{LP} = i_L[(4/\pi D t_{ON}/\delta^2)^{0.5}(1-\gamma)^{1.5} + \gamma]^{-1}$$

i_L is the limiting current density for DC plating. Since the concentration gradient in the pulsating diffusion layer can be very high, and increases with shorter pulse length, the pulse current density can reach extremely high values without a decrease in current efficiency due to hydrogen evolution. As long as the pulse duration time is shorter than the transition time, the average current density used in PC plating will not exceed the DC limiting current density and PC deposits may have a finer grain structure than DC deposits when the same average current density is used.

Sample edge effects in PC plating at average current densities of 2.0, 2.8 and 3.2 mA/cm^2 are shown in Fig. 3. Edge effects are clearly more pronounced at higher current densities. The actual current density at the edge is higher than the current density setting. As the average current density is increased, the actual current density approaches the limiting current density and the deposits are more likely to exhibit microstructures characteristic of limiting current conditions, i.e., coarse grains and even dendritic growth.

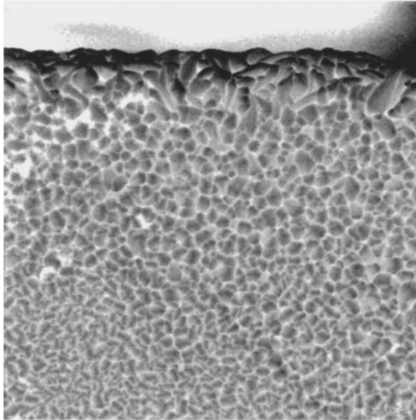

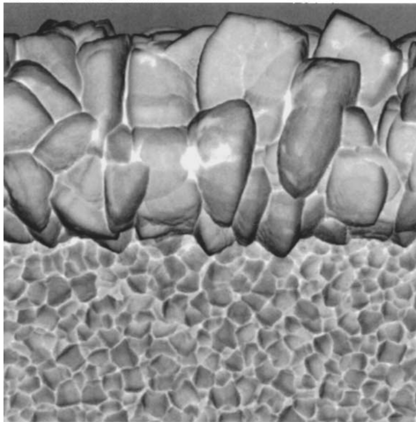

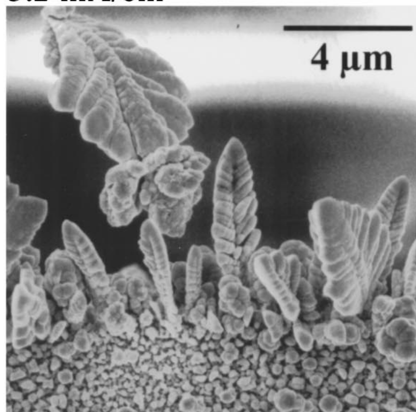

Figure 3 SEM SE images showing edge effects in PC plating at different average current densities. The ON and OFF times for PC plating are 2 ms and 8 ms respectively.

3.2. Effect of ON time

Deposit composition results obtained at different ON times, for a fixed average current density (2.4 mA/cm^2) and cycle period (10 ms), are plotted in Fig. 4. Corresponding microstructures are shown in Fig. 5. The deposit composition plot initially increases with increasing ON time, forms a plateau in the 1–4 ms range and then decreases at values greater than 4 ms. The wide plateau has obvious advantages for practical plating operations. An increase in ON time corresponds to a decrease in the peak current density (since the average current density is fixed) and a decrease in the OFF time. If the ON time is too short, e.g., 0.2 to 0.5 ms, charging or capacitance effects are evident. The faradaic current for alloy plating is substantially lower than the peak current setting, which may explain the lower Sn content. At long ON times, e.g., 5 ms, the peak current density is quite low, which favours Au plating and therefore results in a lower Sn content. For example, at an ON of 5 ms, the peak current density is 4.8 mA/cm^2 which is ≈20% of the peak current density for an ON time of 1 ms.

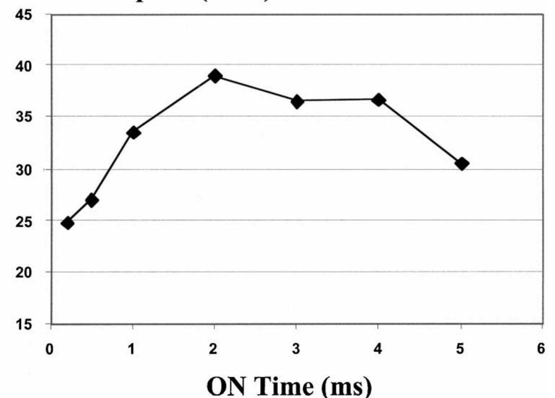

Figure 4 The effect of ON time in PC plating on deposit composition at a constant average current density of 2.4 mA/cm^2 and a cycle period of 10 ms. Error bars are contained within the data points.

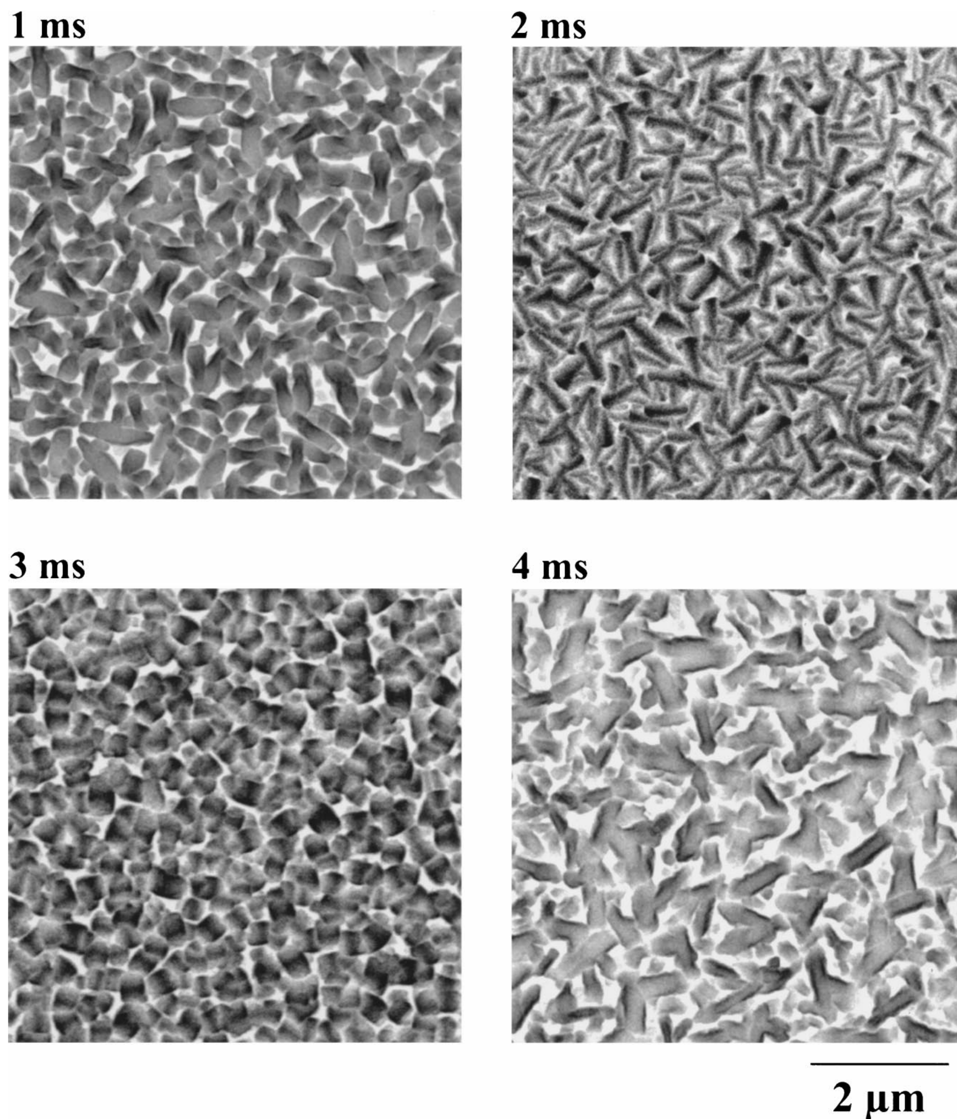

Figure 5 SEM SE images for PC deposits at various ON times at a constant current density of 2.4 mA/cm^2 and a cycle period of 10 ms.

For pure metal pulse plating, the ON time should be shorter than the transition time, otherwise hydrogen evolution or organic decomposition may occur. The transition time τ decreases as the pulse current density I increases according to the following equation (assuming $D\tau/\delta^2 \ll 0.1$).

$$\tau I^2 = (\pi D n^2 F^2/4)C^2$$

F is the Faraday constant (96,500 C) and C is the metal ion concentration. Hydrogen evolution decreases the current efficiency while organic decomposition causing carbon plating destroys the deposit by increasing the deposit resistance. For alloy pulse plating, the mechanism is somewhat more complicated than that for pure metal pulse plating; it is possible that each component has its own transition time.

It is clear from the SEM micrographs in Fig. 5 that deposits obtained at 2 ms of ON time have the densest structures, finest grain size and smoothest deposits. This is confirmed by AFM surface roughness measurements. Deposit surface mean roughness values for 1, 2, 3 and 4 ms ON times are 73.8, 58.4, 64.1 and 62.9 nm, respectively.

Deposit composition results obtained at different ON times, for a constant peak current density (10 mA/cm^2) and OFF time (8 ms), are plotted in Fig. 6. The Sn content increases with increasing ON time for short ON

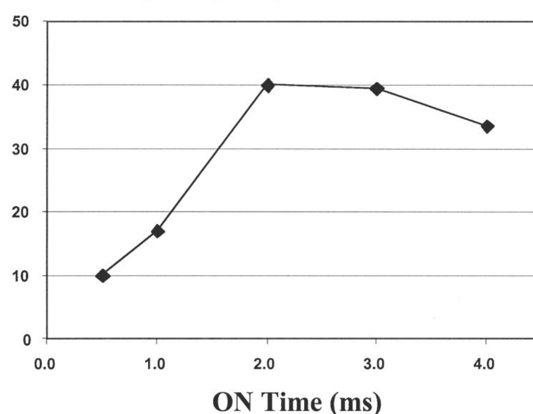

Figure 6 The effect of ON time on deposit composition at a constant peak current density of 10 mA/cm^2 and an OFF time of 8 ms. Error bars are contained within the data points.

times, reaches a plateau and then decreases with further increases in ON time. The rising portion of the curve may be related to the transition time for Au plating. For ON times longer than 0.5 ms, Au plating becomes diffusion controlled and Sn plating or hydrogen evolution begins. As such, the Au transition time is $\leq$0.5 ms. When the ON time is increased to $\approx$2 ms, both Au and Sn plating are likely diffusion controlled, giving rise to the plateau in the composition plot. Further increases in ON time lead to additional hydrogen evolution, which may result in an increase in the local pH value and suppress Sn plating.

SEM micrographs of deposits obtained at different ON times are shown in Fig. 7. The 1 ms ON time sample has a much finer microstructure than the other deposits. This is due in part to its high Au content or low Sn content (16.7 at%) relative to the others, which have Sn levels greater than 33 at%. For the higher Sn content deposits, roughness increases with increasing ON time. At longer ON times, the average current density increases leading to thicker and coarser deposits. At 4 ms of ON time, the microstructure approaches that obtained from DC plating.

Cleaved cross sections of the deposits in Fig. 7 are shown in Fig. 8. The 1 ms ON time sample exhibits ductile fracture, which is due to its high Au content. Deposits obtained at 2 and 3 ms of ON time are dense and uniform and adhere well to the substrate. The microstructures are very similar to typical solidified cast structures, with the initial deposit fine grained and subsequent grains growing in a columnar manner. The fractured surfaces of these two deposits are more characteristic of brittle fracture, due to the increased amount of AuSn; both deposits are hypereutectic in composition, i.e., 39 at% Sn compared to the eutectic value of $\approx$30 at% Sn. The 4 ms ON time sample is very rough - its thickness varies from 1.4 to 8.9 μm - which is due to the high average current density (3.3 mA/cm^2), which is likely close to the limiting current density.

Practically speaking, ON times of 1–3 ms produce suitable microstructures and reasonable plating rates (0.7–1.7 μm/hr). Higher plating rates could be achieved by increasing the Au and Sn contents in the plating bath, which has the effect of increasing the limiting current density.

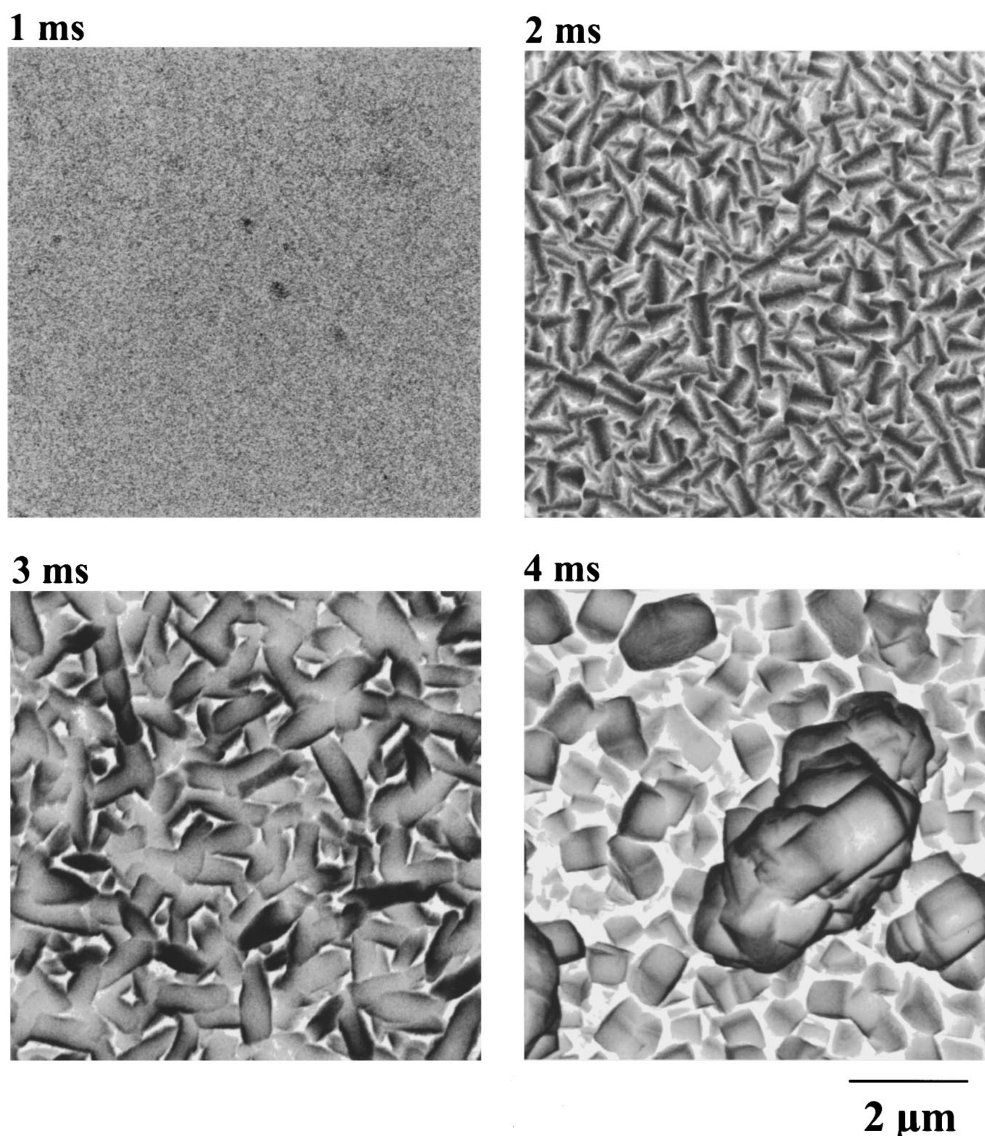

Figure 7 SEM SE images of deposits obtained at different ON times, with a constant peak current density of 10 mA/cm^2 and an OFF time of 8 ms.

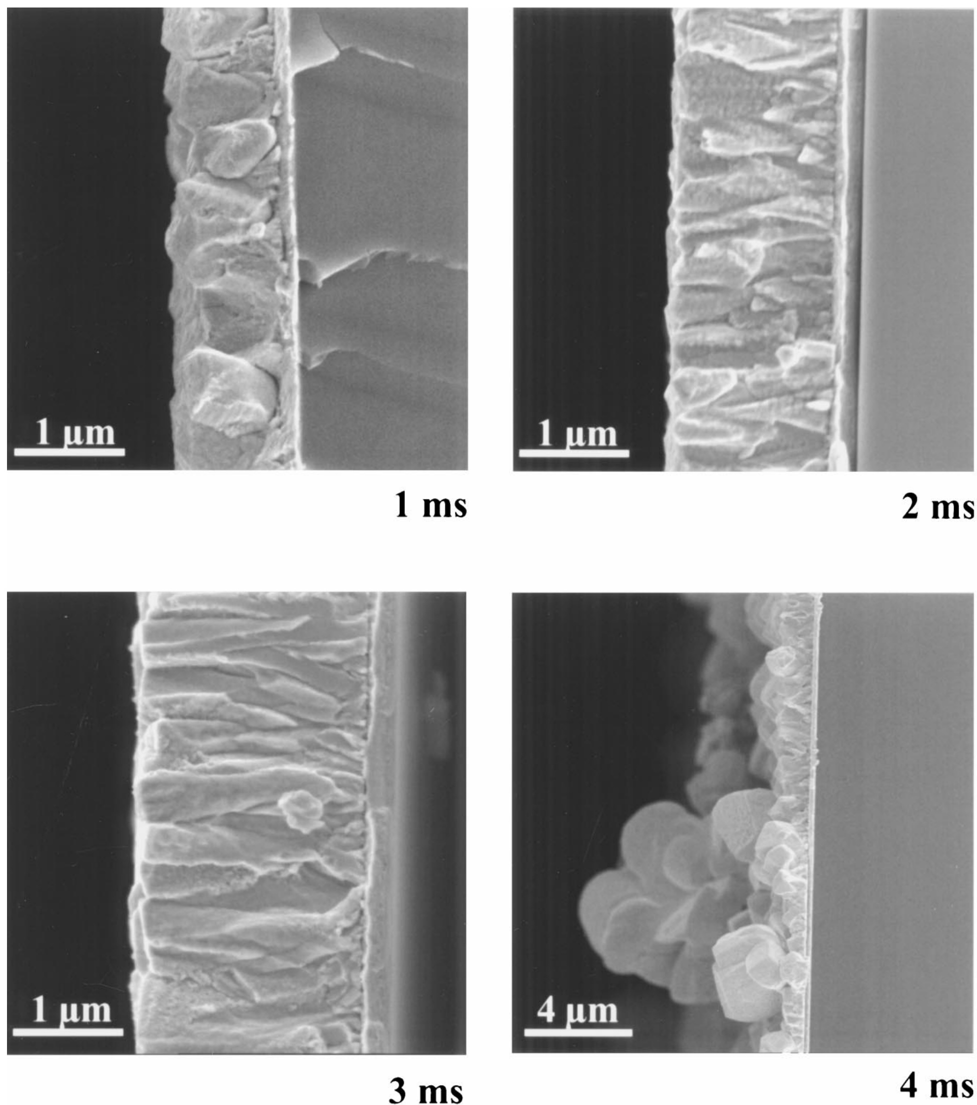

Figure 8 SEM cleaved cross section images of deposits obtained at different ON times, with a constant peak current density of 10 mA/cm^2 and an OFF time of 8 ms.

3.3. Effect of OFF time

The effect of OFF time on deposit concentration is shown in Fig. 9. In all cases, the peak current density was 10 mA/cm^2, the ON time was 2 ms and the plating time was 80 min. The Sn content initially increases for OFF times in the 3–4 ms range; further increases in OFF time lead to a constant Sn content. During the ON portion of the plating cycle, the cathode region becomes depleted of Sn ions. During the OFF time, the Sn ion concentration is recovered to some extent, before the next pulse, by the diffusion of Sn ions from the bulk solution to the depletion region. The extent of recovery depends on the length of OFF time. If the OFF time is long enough ($\approx$4 ms here), the Sn ion concentration at the cathode reaches the bulk value before the next pulse. Any further increase in OFF time has no influence on deposit concentration.

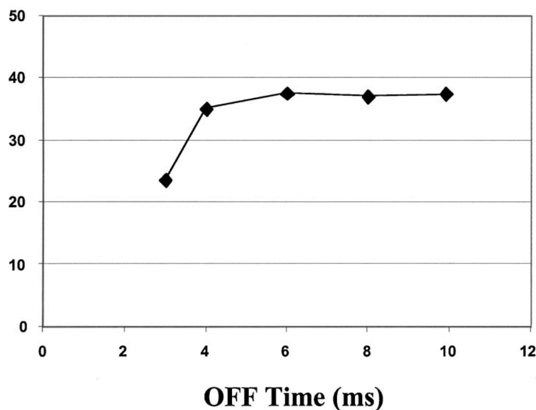

Figure 9 The effect of OFF time on deposit composition. The peak current density is fixed at 10 mA/cm^2 and the ON time is 2 ms. Error bars are contained within the data points.

SEM images corresponding to the deposits plotted in Fig. 9 are shown in Fig. 10. The 3 ms OFF time sample is not shown, but was quite porous and black in colour, which indicates a high carbon content in the deposit. The OFF time was too short to allow the Au and Sn concentrations at the cathode to return to the bulk values, resulting in a diffusion controlled plating condition. For deposits with OFF times $\geq$4 ms, the microstructure becomes finer with increasing OFF time, while the composition remains almost constant. The longest OFF times (8 and 9.9 ms) give similar microstructures, which indicates that the recovery time is sufficient.

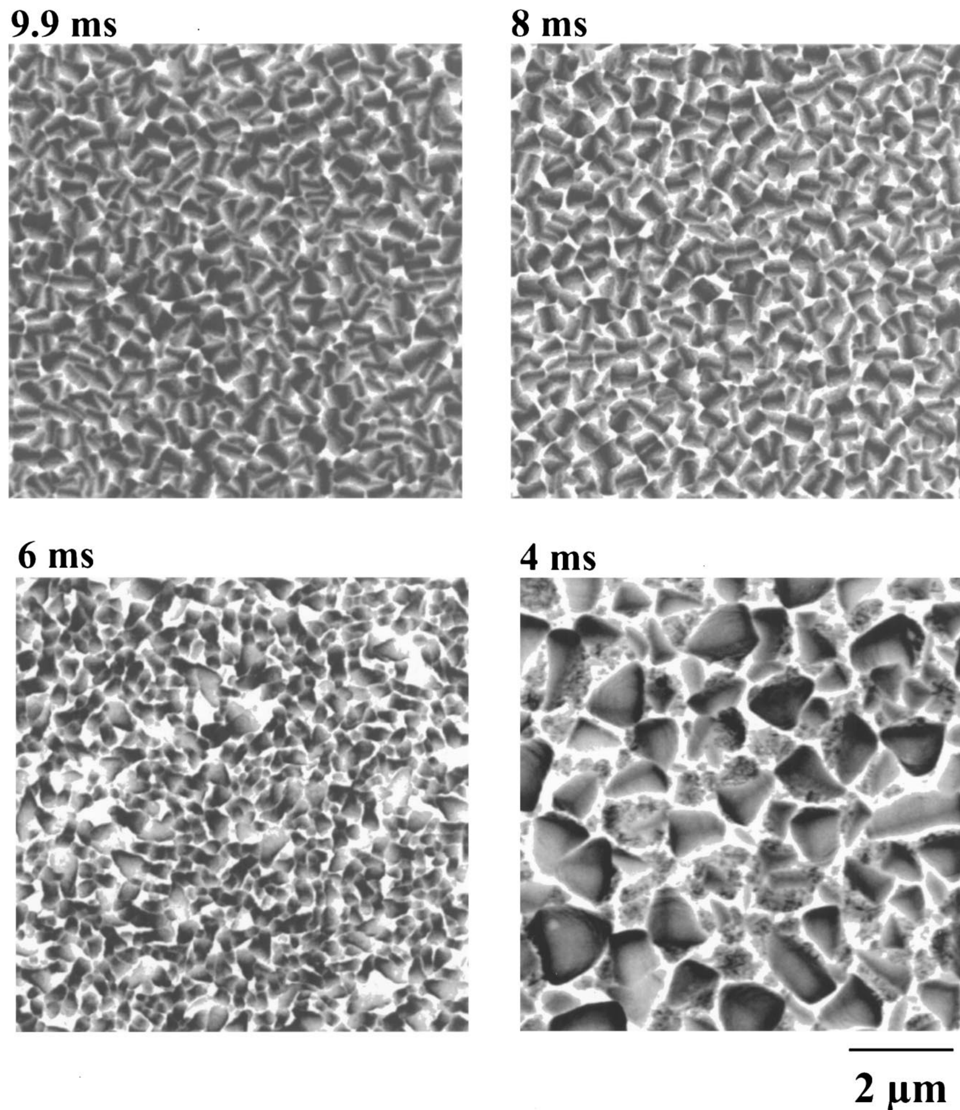

Figure 10 SEM SE images of deposits obtained at different OFF times, with the peak current density fixed at 10 mA/cm^2 and an ON time of 2 ms.

OFF time has been reported to affect deposit microstructure in different ways. An increase in OFF time resulted in grain refinement for Cd deposition, but in grain growth for Cu and Au [19]. It is argued that for Cu and Au, grain growth, which is thermodynamically driven, occurs during the OFF cycle. For Cd, grain growth is believed to be retarded by adsorption of inhibiting species during the OFF cycle.

Cleaved cross section images of samples obtained at OFF times of 9.9 ms and 4 ms are shown in Fig. 11. The thicknesses of the 2 deposits are 1.6 and 7.6 μm respectively. The average current density for the 4 ms OFF time sample is twice that of the 9.9 ms OFF time sample, however, the deposit thickness at 4 ms of OFF time is more than 4 times that of the 9.9 ms OFF time sample. Both samples exhibit a columnar structure, with the 9.9 ms OFF time sample being more dense.

3.4. Reproducibility testing

A single metallized InP wafer piece ($\approx$1.46 cm^2 exposed area) was plated continuously from a 50 ml plating solution to a final thickness of $\approx$26 μm. Surface composition analysis of the resultant deposit at 5 different locations yielded an average composition of 10.8 ± 0.6 at% Sn. The surface morphology was fairly coarse. SEM images of cleaved and polished cross sections are shown in Fig. 12. The deposits are columnar with a finer grain structure near the metallization layer (Fig. 12a). The fracture mode of the cleaved sections is primarily brittle in nature, but becomes more ductile near the deposit surface. This is an indication that the composition is more Sn-rich in the interior of the deposit and Sn-deficient near the surface.

A backscattered electron (BSE) image of a polished cross section is shown in Fig. 12b. The image contrast (due to atomic number effects) is more pronounced for the BSE images relative to the SE images, with the columnar behaviour clearly evident. Sn-rich regions are darker, while the lighter contrast regions are Au-rich. The BSE images show 2 distinct layers. The inner layer consists of 2 phases and is $\approx$23 μm thick, while the outer layer (2–3 μm thick) appears to be a single phase and Au-rich. The Au-rich outer layer corroborates the EDX analysis done on the surface of the deposit. Composition depth profiles (at 2.25 μm intervals)

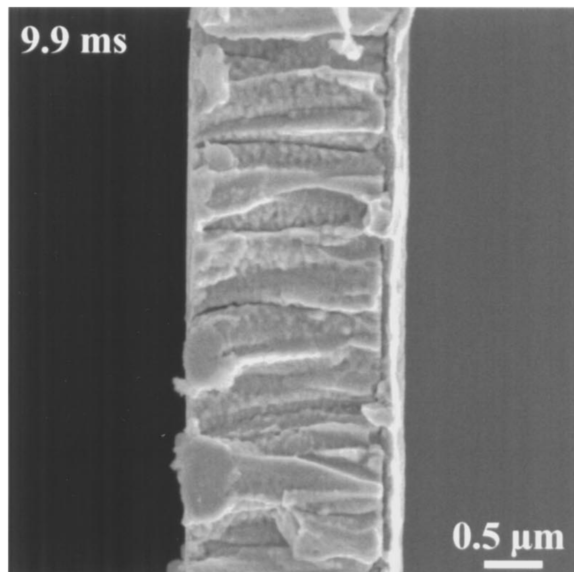

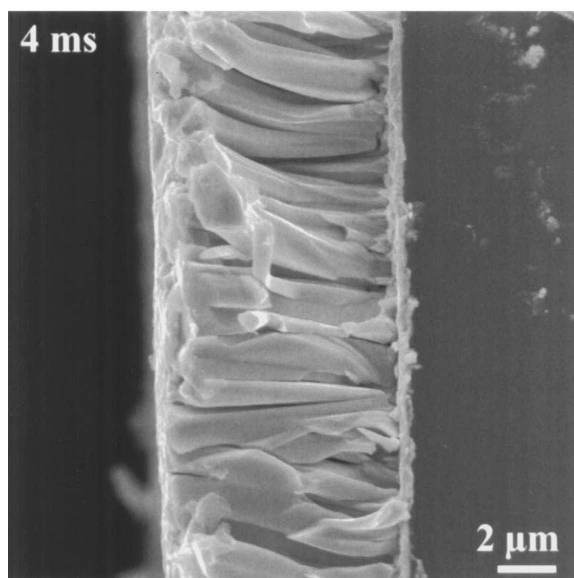

Figure 11 SEM cleaved cross section images of deposits obtained at OFF times of 9.9 ms and 4 ms. The peak current density was fixed at 10 mA/cm^2 and the ON time was 2 ms.

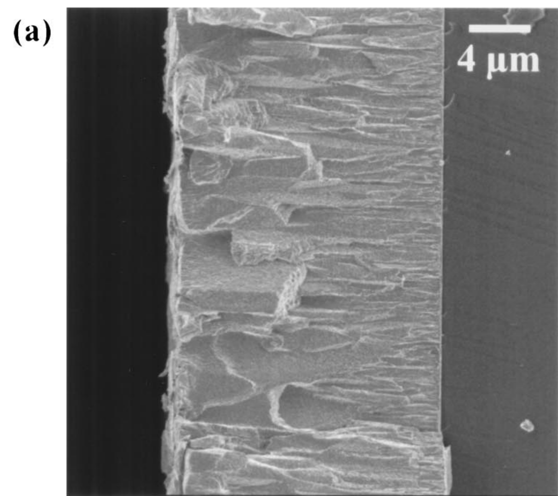

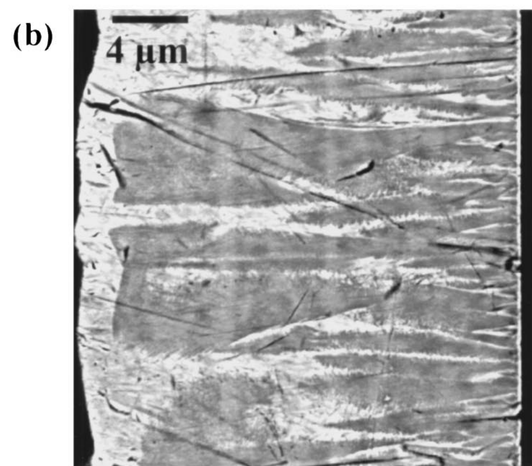

Figure 12 (a) SEM SE image of a cleaved cross section of the deposit produced from the reproducibility test. (b) SEM backscattered electron (BSE) image from a polished cross of the same sample. The semiconductor substrate is to the right of the deposit.

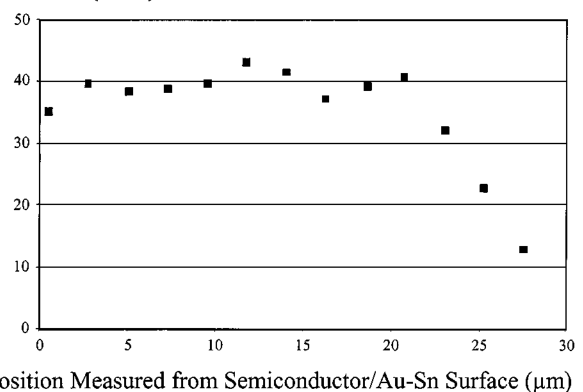

Figure 13 Composition depth profile for the sample shown in Fig. 12. Four individual profiles have been summed and averaged.

at 4 locations were done through the thickness of the deposit. Because of local variations in composition, due primarily to presence of 2 distinctly different phases, the profiles were summed and plotted as a single profile (Fig. 13). The resultant composition profile correlates well with the cross section images, i.e., up to 22–23 μm of Au/Sn solder of uniform composition can be deposited from a single 50 ml solution.

Based on the above information, the number of InP wafers (2 inch diameter) that could be plated from the same bath without a significant composition change was estimated. If the process was scaled up to a 2 L plating solution and 3.5 μm of solder was deposited on each wafer, then a total of $\approx$19 wafers could be plated before replenishing the bath.

The percentage of Au in the bath consumed after plating $\approx$22 μm of solder (before the Sn content decreases) can be estimated by assuming the density of the deposit is equal to the bulk density of an equilibrium alloy consisting of Au_5Sn and AuSn. The total volume V of the deposit is the product of the plated area (1.46 cm^2) and the deposit thickness ($\approx$22 μm). Since the average composition of the deposit is Au-39 at% Sn (Au-28 wt% Sn), the volume percentage of Au_5Sn and AuSn in the deposits is $\approx$35% and 65%

respectively. The deposit density ρ_d can be estimated from a weighted average of the densities of Au_5Sn and AuSn, yielding a value of $\approx$13.6 g/cm^3. If g_{Au} is the total weight of Au added to the bath prior to plating, then the percentage of Au consumed after plating 22 μm of solder is

$$(V\rho_d \text{ wt\% Au}_{\text{deposit}})/g_{\text{Au}} \approx 24 \text{ wt\%}$$

The percentage of Sn consumed can be calculated in a similar manner and amounts to $\approx$8.5 wt%. The Au content in the plating solution has changed significantly, while the Sn content has only changed a small amount.

Decreasing Sn content with increasing plating time has been addressed by Holbrom *et al.* [21], who attributes it to faster Sn consumption due to the formation of Sn-rich agglomerates. This explanation is reasonable for a large current density which is close to the limiting current density. For this work, the current density is 1.6 mA/cm^2, which is significantly lower than the limiting current density of $\approx$4 mA/cm^2. The change in deposit composition with plating time may instead be due to composition changes in the solution additives.

3.5. Summary

A relatively stable, non-cyanide, weakly acidic solution has been utilized to co-electroplate Au-Sn alloys onto metallized semiconductor substrates. Depositions were done under both DC and PC conditions and the results are summarized in the following.

- In the studied range of average current density, PC deposits have consistently higher Sn content than DC deposits. At low current densities ($<$2.4 mA/cm^2), the microstructures are similar, while at higher current densities, PC deposits are finer and smoother.
- For PC plating, when the average current density and cycle period are held constant, the composition vs ON time plot shows a plateau. Deposits obtained at 2 ms of ON time, which is within the plateau region, have the finest and smoothest microstructure. When the peak current density and OFF time are held constant, a plateau is also observed in the deposit composition vs ON time curve. Grain structures are finer for shorter ON times.
- When the peak current density and ON time are held constant, the Sn content in the deposits first increases with increasing OFF time and then reaches a plateau. Short OFF times (3–4 ms) give coarse grained microstructures, while longer OFF times (6–9.9 ms) give consistently uniform microstructures.
- Reproducibility tests indicate that several 2 inch wafers ($>$10) could be electroplated with Au-Sn solder ($\approx$39 at% Sn) to a thickness of 3.5 μm.

Acknowledgements

This work was funded by grants from Nortel Technology and the Natural Sciences and Engineering Research Council (NSERC) of Canada.

References

1. H. JONES, "Rapid solidification of Metals and Alloys," (Institute of Metallurgists Monograph, No. 8, London, 1982).
2. C. C. LEE, C. Y. WANG and G. S. MATIJASEVIC, *IEEE Transactions Comp. Hybrids, Manufacturing Technology* **14** (1991) 407.
3. A. KATZ, C. H. LEE and K. L. TAI, *Materials Chemistry and Physics* **37** (1994) 303.
4. W. PITTROFF, T. REICHE, J. BARNIKOW, A. KLEIN, U. MERKEL, K. VOGEL and J. WURFL, *Applied Physics Letters* **67** (1995) 2367.
5. O. WADA, in Materials Research Society Symposium Proceedings, (1992) Vol. 260, p. 713.
6. G. R. DOHLE, J. J. CALLAHAN, K. P. MARTIN and T. J. DRABIK, *IEEE Transactions Comp. Packaging and Manufacturing Technology, Part B* **19** (1996) 57.
7. D. G. IVEY, *Micron* **29** (1998) 251.
8. F. R. SCHLODDER, H. H. BEYER and W. G. ZILSKE, in Proceedings of the Symposium on the Industrial Uses of Gold, (SAIMM, Johannesburg, South Africa, 1986) Vol. 3, p. 21.
9. C. KALLMAYER, D. LIN, J. KLOESER, H. OPPERMANN, E. ZAKEL and H. REICHL, in IEEE/CPMT International Electronics Manufacturing Technology Symposium (1995) p. 20.
10. C. KALLMAYER, D. LIN, H. OPPERMANN, J. KLOESER, S. WEIB, E. ZAKEL and H. REICHL, in 10th European Microelectronics Conference (1995) p. 440.
11. C. KALLMAYER, H. OPPERMANN, J. KLOESER, E. ZAKEL and H. REICHL, in Proceedings ITAP, San Jose, 1995.
12. T. FREY, T. W. HEMPEL and G. HERKLOTS, "Bright gold-tin alloy electroplating bath- has long term stability without use of soluble tin anode," DE 4406434, 1995.
13. S. MATSUMOTO and Y. INOMATA, "Gold-tin alloy plating bath and method," Japanese Kokai Tokkyo Koho JP 61 15, 992, 1986.
14. D. G. FOULKE and R. DUVA, in Plating in the Electronics Industry, 4th Symposium (Indianapolis, Indiana, 1973) p. 131.
15. N. KUBOTA, T. HORKOSHI and E. SATO, *Journal of Met. Fin. Soc. Japan* **34** (1983) 37.
16. Y. TANABE, N. HASEGAWA and M. ODAKA, *Journal of the Metallurgical Society of Japan* **34** (1983) 452.
17. R. J. MORRISSEY, *Plating and Surface Finishing* **80** (1993) 75.
18. A. KNODLER, in "Theory and Practice of Pulse Plating," edited by J. Puipe and F. Leaman (American Electroplaters and Finishers Society, 1986) Ch. 9, p. 119.
19. J. C. PUIPE, in "Theory and Practice of Pulse Plating," edited by J. Puipe and F. Leaman (American Electroplaters and Finishers Society, 1986) Ch. 3, p. 1.
20. N. IBL, *Surface Technology* **10** (1980) 81.
21. G. HOLMBOM, J. A. ABYS, H. K. STRASCHIL and M. SVENSSON, *Plating and Surface Finishing* **85** (1998) 66.

Received 14 May 1999
and accepted 3 August 2000